# Three-dimensional (3D) reconstructions of the coastal cliff face in Normandy (France) based on oblique Pléiades imagery: assessment of Ames Stereo Pipeline® (ASP®) and MicMac® processing chains

Pauline Letortu, Roza Taouki, Marion Jaud, Stéphane Costa, Olivier Maquaire, Christophe Delacourt

Letortu P., Jaud M., Taouki M, Costa S., Maquaire O., Delacourt C., 2021. Three-dimensional (3D) reconstructions of the coastal cliff face in Normandy (France) based on oblique Pléiades imagery: assessment of Ames Stereo Pipeline® (ASP®) and MicMac® processing chains. *International Journal of Remote Sensing*. https://doi.org/10.1080/01431161.2021.1892857

# Three-dimensional (3D) reconstructions of the coastal cliff face in Normandy (France) based on oblique Pléiades imagery: assessment of Ames Stereo Pipeline® (ASP®) and MicMac® processing chains

Pauline Letortu[a]*, Roza Taouki[a], Marion Jaud[b], Stéphane Costa[c], Olivier Maquaire[c] and Christophe Delacourt[d]

*[a]University of Western Brittany, IUEM, CNRS, UMR 6554 – LETG, Plouzané, France, pauline.letortu@univ-brest.fr, roza.taouki@univ-brest.fr; [b]University of Western Brittany, IUEM, CNRS, UMS 3113 – IUEM, Plouzané, France, marion.jaud@univ-brest.fr; [c]Normandy Univ, UNICAEN, CNRS, UMR 6554 – LETG, Caen, France, stephane.costa@unicaen.fr, olivier.maquaire@unicaen.fr; [d]University of Western Brittany, IUEM, CNRS, UMR 6538 – LGO, Plouzané, France, christophe.delacourt@univ-brest.fr*

Letortu P., Jaud M., Taouki M, Costa S., Maquaire O., Delacourt C., 2021. Three-dimensional (3D) reconstructions of the coastal cliff face in Normandy (France) based on oblique Pléiades imagery: assessment of Ames Stereo Pipeline® (ASP®) and MicMac® processing chains. *International Journal of Remote Sensing*. https://doi.org/10.1080/01431161.2021.1892857

# Three-dimensional (3D) reconstructions of the coastal cliff face in Normandy (France) based on oblique Pléiades imagery: assessment of Ames Stereo Pipeline® (ASP®) and MicMac® processing chains

Images from agile (viewing angle over 40°) and very high spatial resolution satellites (inferior to 1 m) can be useful for monitoring cliff faces, which is the best proxy to better understand coastal cliff dynamics. However, these images with a specific configuration are rarely used, partly because it is cumbersome to process them. Based on Pléiades images of the coastal cliff face along the coast of Normandy, with a high angle of incidence (up to 40°) and taken on multiple dates, the paper aims to identify i) the best open-source processing chain to reconstitute three-dimensional (3D) cliff faces by stereo restitution ii) the reasons behind its best performance and iii) the key parameters to change depending on the image datasets or processing chains so as to facilitate transposition. The Ames Stereo Pipeline® (ASP®) and MicMac® software programmes were tested using different parameters (matching algorithm, size of correlation window, etc.) for the 3D reconstructions. MicMac® provides the best performance using GeomImage (1-2 pixel matching) with a size of correlation window of 3 × 3 or 7 × 7 associated with a regularization parameter of 0.10. With these parameters, the point clouds of the cliff face have an average point density of 1.70 point $m^{-2}$, a mean distance from Unmanned Aerial Vehicle (UAV) ground truth data of 0.04 m and a standard deviation of 1.72 m. With these characteristics, the threshold of rockfall detection using a multi-source comparison is assessed at 100 $m^3$, which involves that the large majority of rockfalls (69%) around the study area could be detected by a diachronic approach. Considering the daily Pléiades revisiting time, this method offers a great opportunity to monitor erosion and to better understand coastal cliff dynamics.

Keywords: Pléiades satellites, oblique images, 3D restitution, cliff face, coastal erosion.

## Introduction

Starting in the 2000s, the new generations of very high spatial resolution (less than 1 m in panchromatic mode) and agile satellites with short revisit time (QuickBird, WorldView, GeoEye, Pléiades, until around 40°) offer a greater scientific potential to combine large scale, high-resolution studies (Poli et al. 2015; Collin et al. 2018), and to do three-dimensional (3D) topographic reconstructions from pairs or triplets of images from different viewing angles. Some topics in geosciences have explored the potential of these new datasets. Elevation changes in glacier topography can be studied thanks to

Pléiades stereo imagery (Berthier et al. 2014), height changes due to earthquakes can be determined by stereo and tri-stereo reconstructions with a precision of a few decimetres (Zhou et al. 2015), lava flow volume can be estimated with Digital Elevation Model (DEM) of Difference (DoD) computed from Pléiades triplet images (Bagnardi, González, and Hooper 2016).

To observe all the changes of the coastal cliff, the entire cliff face (from the foot of the cliff to its top) should be observed. This means that the best point of view is horizontal. However, cliff face surveys are quite rare given that few datasets use this point of view. Until recently, most datasets had a vertical point of view (aerial photographs, aerial Light Detection And Ranging (LiDAR), satellite imagery, etc.), and therefore the most common proxy to determine the evolution of the cliff was the cliff top (e.g. Costa 1997; Zviely and Klein 2004; Foyle and Naber 2012). The arrival of agile (i.e. satellites able to observe the field from a high angle of incidence) and very high spatial resolution satellites, Terrestrial Laser Scanners (TLS), terrestrial photogrammetry, mobile laser scanners set up on a boat have made it easier to observe the cliff face and therefore to record its changes (e.g. Letortu et al. 2020; Gulyaev and Buckeridge 2004; Letortu et al. 2018; Michoud et al. 2014, respectively). Whereas i) coastal cliffs likely exist on roughly 52% of the global shoreline (Young and Carilli 2019) ii) many people, houses, companies, infrastructure are/could be threatened by the risk of coastal erosion iii) there are high societal and political demands for reliable, homogeneous, perennial and low-cost data on long stretches of coastline in order to better understand erosion and protect inhabitants iv) various agile and very high spatial resolution satellites are available (e.g. QuickBird, GeoEye, WorldView and Pléiades), this research topic is still in its early stages with a unique paper (Letortu et al. 2020).

Pléiades-HR (High-Resolution Optical Imaging Constellation) is a two-spacecraft constellation of CNES (the French Space Agency). The Pléiades 1A and 1B satellites were launched (16 December 2011, 02 December 2012, respectively) by the Soyuz launcher from the French Guiana Space in Kourou. The Pléiades satellites have six main qualities that are useful for coastal cliff studies (ASTRIUM 2012):

(1) The very high spatial resolution of their images (e.g. a ground sampling distance of 0.70 m at the nadir for panchromatic images);
(2) A high level of agility, with a theoretical viewing angle up to 47°;
(3) The daily revisit frequency;
(4) A swath width of 20 km at the nadir, in line with the coastal management scale, i.e. the hydro-sedimentary cell (from hundreds of metres to hundreds of kilometres);
(5) A mission lifetime of ten years and a continuity of measurements between the next versions of the satellites (Pléiades Neo constellation);
(6) Free access to the images under certain conditions for research institutes.

The EROFALITT (erosion of coastal cliffs) project was funded by CNES (2016-2020) in order to explore the potential of Pléiades images to monitor the evolution of coastal cliffs by observing the cliff face proxy. With Pléiades images with a high angle incidence, 3D reconstitutions of cliff faces along the coast of Normandy (NW France) were performed. This project was challenging because:

- It is located in Varengeville-sur-Mer (Seine-Maritime), where disturbed weather and the NNE orientation of the cliff face can alter the image quality (due to clouds and shadows, respectively);

- It has uncommon image acquisition modalities: because of the NNE orientation of the cliff face, it was shown that the standard stereo or tri-stereo acquisition was unsuitable. Another acquisition modality was proposed: a multi-date survey over several consecutive days. As the orbital pass position of the Pléiades satellites changes daily, a mono-acquisition up to an incidence angle of 40° (across-track) acquired on successive days (around 13:20 in local time, Universal Time Coordinated (UTC) + 2) can be used to observe the cliff face at various viewing angles to reconstruct it in 3D via stereo restitution. To assess the impact of the angle of incidence, two sets of images were simultaneously requested each day: one with a pitch imaging angle of 40° and a second one with a pitch imaging angle between 0° and 10° (more details in Letortu et al. 2020);
- There is a limited choice of image processing software programmes as this is an unusual image dataset.

The objectives of this paper are to answer two main questions:

- What is the best processing chain to obtain a 3D reconstitution of the cliff face between Ames Stereo Pipeline® (ASP®) and MicMac® from our image dataset? Why?
- What are the key parameters that depend on the images or the processing chain per software in order to facilitate any transposition of our method to other sites or images (no need to test all the parameters, but only a few)?

A high angle of incidence and multi-date images acquired by a push broom sensor limit the number of software programmes that can be used to process images (e.g. ASP®, ERDAS IMAGINE®, Satellite Stereo Pipeline® (S2P®), MicMac®, Agisoft

Metashape®). Previously, we used ERDAS IMAGINE® (Letortu et al. 2020); however open-source software and well-documented processing were important criteria in our choice of which software to test. Our goal is to understand why one software package or processing parameter works better than another, therefore we must avoid the 'black box' effect. Consistent with these requirements, we selected the ASP® (https://ti.arc.nasa.gov/tech/asr/groups/intelligent-robotics/ngt/stereo/; Shean et al. 2016) and MicMac® (https://micmac.ensg.eu/; Rupnik, Daakir, and Pierrot Deseilligny 2017) software programmes and the test will focus on the parameters used in stereo matching algorithms. The tests are based on the best images in our set acquired in June and July 2017 with pitch imaging angles of 40° and between 0° and 10° (Letortu et al. 2020).

First, the material and methods including the study area will be described, then the results of our software and processing chain comparison will be presented and discussed.

## Materials and methods

### *Study site*

Located in Normandy (Seine-Maritime, NW France) along the English Channel, Varengeville-sur-Mer (1°00'27.34"E; 49°54'59.77"N) is characterized by sub-vertical coastal cliffs (70° to 90°) carved in Upper Cretaceous chalk with flints (part of the Paris Basin; Pomerol et al. 1987; Mortimore et al. 2004). The study area stretches over 600 m, extending 300 m on both sides of the dry valley, called Petit Ailly (Figure 1). These cliffs are mainly white in colour (chalk), but are darkened (brown colour) by a bed comprised of clay and sand sediment from the Tertiary Period (Palaeogene). These cliffs are very prone to erosion (0.36 m $year^{-1}$ between 2010 and 2017 (Letortu et al.

144 2019) whereas the average county retreat rate is 0.15 m year$^{-1}$ (between Cap d'Antifer
145 and Le Tréport, during the 1966-2008 period (Letortu et al. 2014)), with many rockfalls
146 of several cubic metres to hundreds of thousands of cubic metres (Letortu et al. 2015).
147 A fatality occurred in August 2015 in Varengeville-sur-Mer due to falling rocks.

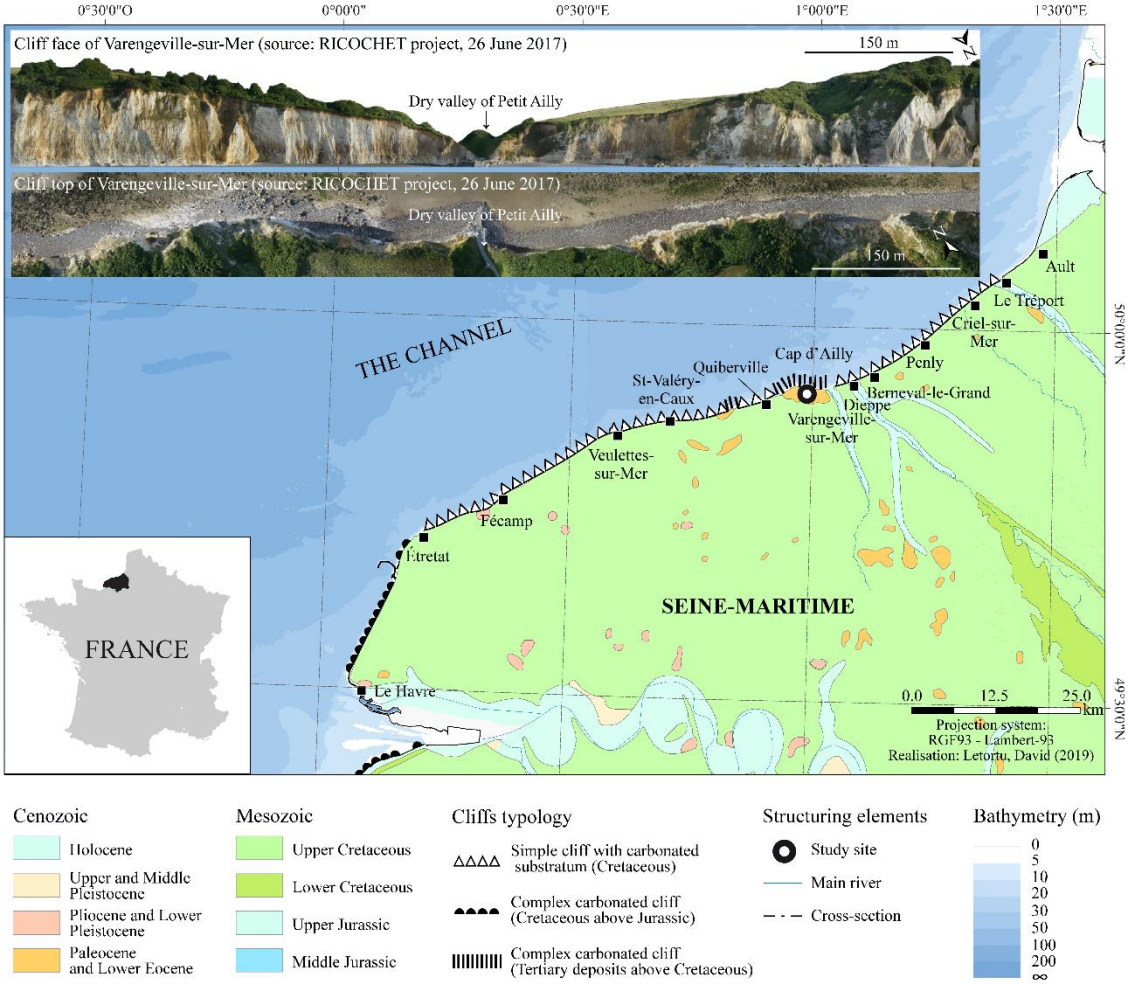


148

149 Figure 1. Presentation of the study area of Varengeville-sur-Mer (Seine-Maritime,
150 Normandy, France).

151

152 Climatically, the study area belongs to the western part of Europe, which is
153 particularly exposed to the influences of low oceanic pressures, and thus, to the types of
154 disturbed weather that dominate approximately 2/3 of the year (Pédelaborde 1958;
155 Trzpit 1970).

156 The average tidal range is 8 m (macrotidal environment). At low tide, the
157 foreshore is characterized by a wide shore platform slightly inclined to the sea covered
158 by sand and with a gravel barrier near the contact with the cliff foot. The average
159 altitude of the Varengeville-sur-Mer cliffs is approximately 30 m and the coastline is
160 relatively jagged due to rockfall scars that exploit pre-existing fracturing. The cliff face
161 is oriented toward the NNE (Figure 1).

162 This site, found on both sides of the dry valley of Petit Ailly, was chosen
163 because the cliff dynamics are frequently monitored (e.g. Costa et al. 2019; Letortu et
164 al. 2019). Since 2010, it is surveyed by terrestrial laser scanners (3 to 4 times a year),
165 Unmanned Aerial Vehicle (UAV) (up to once a year), and aerial topo-bathymetric
166 LiDAR (every 3 years). Since 2014, it belongs to the French Observation National
167 Service DYNALIT (coastal dynamics), which encompasses various coastal sites of
168 scientific interest to better understand the coastal dynamics.

169 The acquisition of oblique and multi-date images from satellites in this study
170 area is challenging for four reasons:

171 (1) cloudy and rainy weather is frequent because it is located in mid-latitudes where
172 disturbed weather dominates, and therefore it can be rare to have good
173 conditions for image acquisition;
174 (2) while the Pléiades satellites have a meridian orbit, the NNE orientation of the
175 cliff face makes it difficult to acquire the image;
176 (3) the cliff face is sub-vertical (70° to 90°) and, due to its orientation, it is in the
177 shadow cast by the cliff at the time the satellite passes over, even during summer
178 (Figures 2 and 3);
179 (4) a high tidal range may hide the cliff foot whereas the whole cliff face is needed.

***Data***

Images were acquired in autumn 2016 (four stereoscopic pairs), in summer 2017 (five stereoscopic pairs) and in winter 2017/2018 (five stereoscopic pairs), covering the 20 km-long cliff line from Quiberville to Berneval-le-Grand (Figure 1). Out of these 28 images, the most relevant stereoscopic pairs for the 3D reconstitution are from June to July 2017 as the weather was sunny and there were few shadows on the cliff face (Letortu et al. 2020).

We decided to focus on six relevant images (10 June 2017, 15 June 2017, 06 July 2017 with incidence angles of 0° to 10° and 40°) and therefore we reduced the study area to only around the dry valley of Petit Ailly at Varengeville-sur-Mer (600 m long), where validation data are available. Over this spatially limited area, a large number of tests on the image processing workflow can be considered in terms of computing resources and computing time (Figures 2 and 3).

| Image date | Local time of satellite pass (UTC+2) | Solar zenith angle (°) | Image incidence angle (°) |
|---|---|---|---|
| 10 June 2017 and 15 June 2017 | 13:20 and 13:31 | 62.1 and 62.9 | 40 |
| 10 June 2017 and 15 June 2017 | 13:21 and 13:33 | 62.2 and 62.7 | 0 to 10 |
| 10 June 2017 | 13:21 and 13:20 | 62.2 and 62.1 | 0 to 10 and 40 |
| 15 June 2017 | 13:33 and 13:31 | 62.7 and 62.9 | 0 to 10 and 40 |
| 15 June 2017 and 06 July 2017 | 13:31 and 13:20 | 62.9 and 61.5 | 40 |
| 15 June 2017 and 06 July 2017 | 13:33 and 13:21 | 62.1 and 61.5 | 0 to 10 |

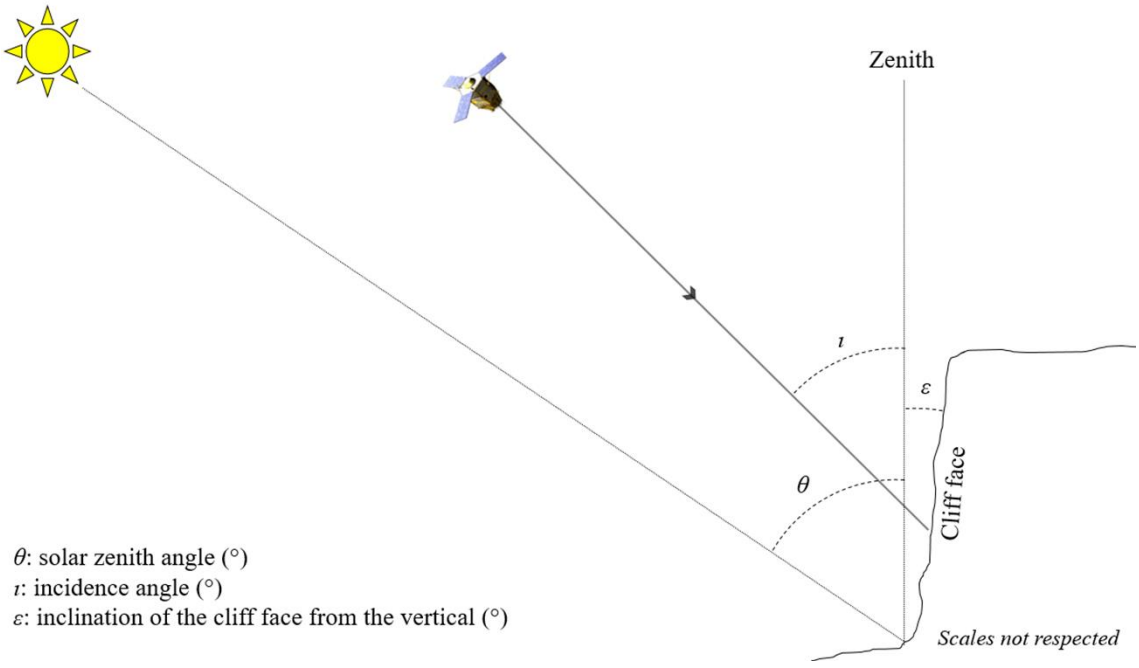


Figure 2. Date, local time of satellite pass, solar zenith angle, and incidence angle of the images selected for the tests.

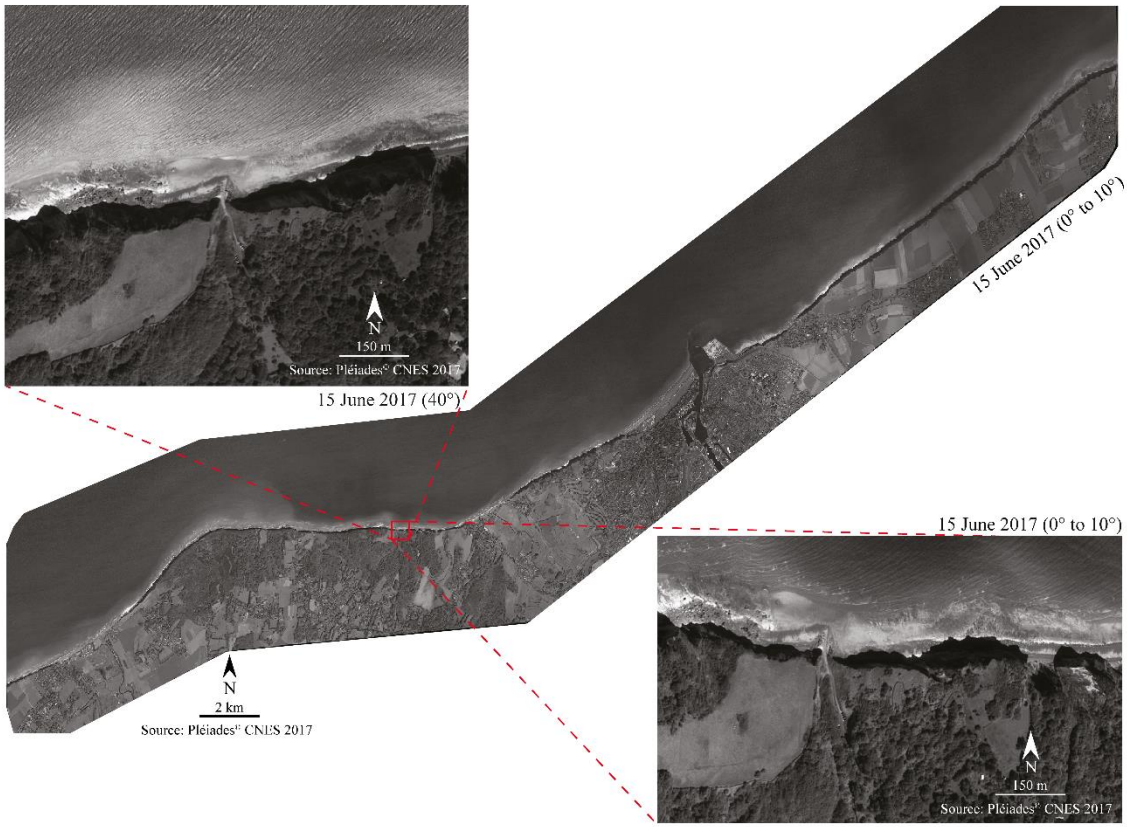


Figure 3. Complete spatial extent of the Pléiades panchromatic image (wavelengths between 470 and 830 nm of the visible spectrum) acquired on 15 June 2017 (0° to 10°) and cropped images around the study area in Varengeville-sur-Mer with incidence angles of 0° to 10° and 40°.

Ground truth data in this paper are from the UAV 3D reconstruction. This survey was ordered for the RICOCHET (multi-risk assessment on coastal territory in a global change context) project and performed by Azur Drones company on 26 June 2017. With a Sony A7R – 36 Mp sensor mounted on an octocopter Mikrokopter, image acquisition were oblique with manual framing. The 3D reconstruction was based on 1740 photographs (spatial extent of about 400 m on both sides of the dry valley of Petit Ailly) and 11 targets located to the ground and measured by Differential Global Positioning System (DGPS). It was projected in an absolute coordinate system, in Lambert-93 and associated Réseau Géodesique Français 1993 (RGF93) and

Nivellement Général de la France-Institut Géographique National69 (NGF-IGN69), which is the official reference system in France (European Petroleum Survey Group (EPSG) registry: 2154). The 3D reconstruction error was of 2.11 cm, with a sampling distance of 3 cm.

TLS ground truth data are also used in this paper. The raw TLS point cloud was obtained from a RIEGL VZ-400 (laser pulse in the near-infrared (1550 nm)) on 25 September 2015, which provides scan data acquisition with theoretical 0.005 m accuracy and 0.003 m precision at a range of 100 m (RIEGL Laser Measurement Systems 2014). In Varengeville-sur-Mer, two scanner stations (located at about 75 m from the cliff face) provided each a dense 3D point cloud (more than 22.5 million points). Twenty-one reflective targets (10 cm high cylinders) with different distances from the scanner were used to georeference the point cloud because they were measured by a total station (Trimble M3). The point cloud (spatial extent of about 150 m on both sides of the dry valley of Petit Ailly) was thus projected in Lambert-93 and associated RGF93 and NGF-IGN69. The TLS data processing encompassed three steps : i) georeferencing and point cloud assembly (RiscanPRO®) ii) manual point cloud filtering including areas without overlap with previous TLS data, noise and vegetation (Fledermaus®) and iii) Delaunay two-and-a-half-dimensional (2.5D) meshing (best fit plane, Cloudcompare®) (more details in Letortu et al. 2018). The 2.5D mesh was used for dataset comparison.

Both methods proved to be relevant in coastal cliff erosion studies thanks to their high resolution and their centimetre precision (Letortu et al. 2018).

## ***Methods***

### *Software packages*

235 The image processing workflow of each software mainly follows the traditional stereo
236 restitution steps for 3D reconstructions (Figure 4): input data, cropped data, image
237 alignment, correlation and 3D point cloud generation (NASA 2019; Rupnik et al. 2020).

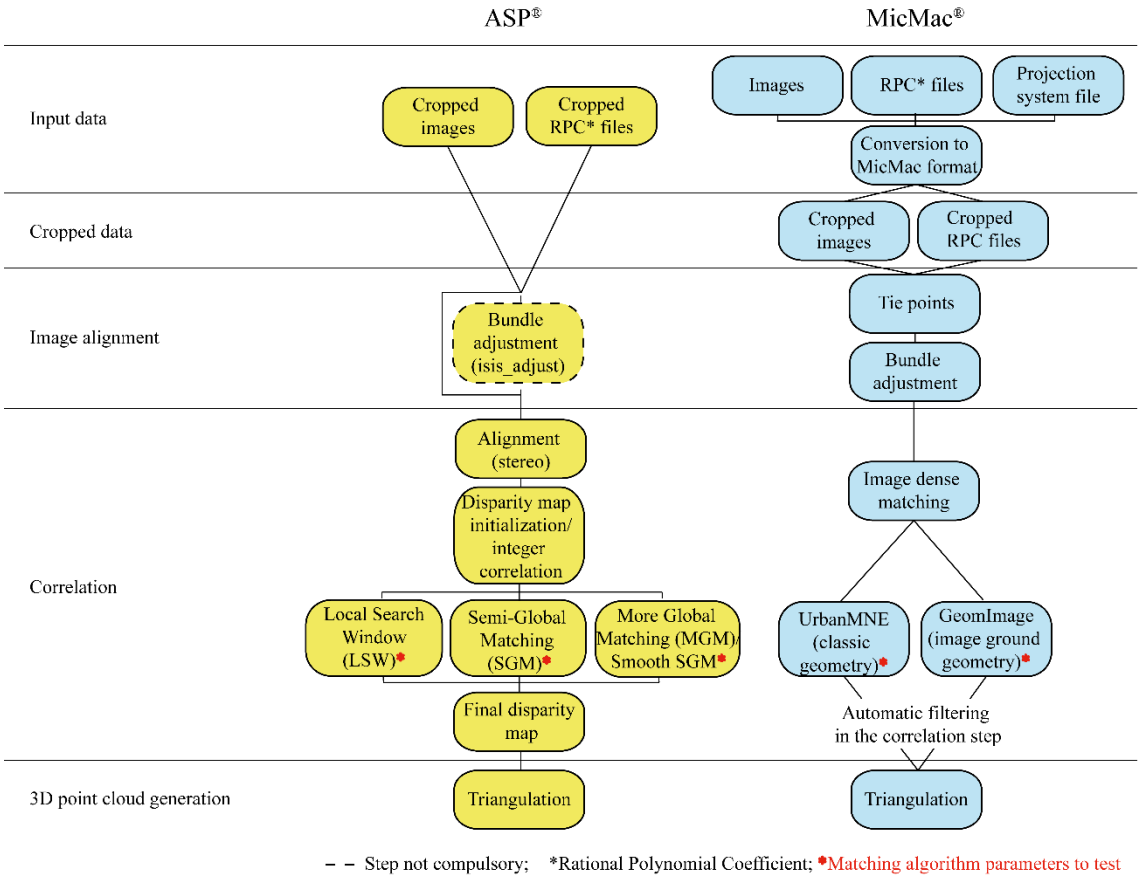


238

239 Figure 4. Image processing workflow of ASP® and MicMac® to obtain a 3D point cloud
240 (NASA 2019; Rupnik et al. 2020).

241

242 Since the images are taken from different viewpoints, the apparent motion of the
243 scene between the views is computed (called “disparity” in the case of stereo-rectified
244 image pairs) (Hartley and Zisserman 2003). Stereo matching in the correlation step is
245 the core of the image processing workflow (Figure 4). It involves identifying pixel
246 correspondences between the left and right epipolar images. Our tests focused on this
247 correlation step, which is different between ASP® and MicMac®.

In ASP®, three matching algorithms are possible (Figures 4 and 5):

- Local Search Window (LSW), which is the default ASP® correlation algorithm. A disparity value is computed by correlation for each valid pixel identified in the input image. As the search window size is a key parameter of the correlation step and in order to be efficient in larger search ranges, a Gaussian pyramid approach is applied, that is to say disparities are first estimated using sub-sampled images, and are gradually refined at higher resolution.
- Semi-Global Matching (SGM), introduced in Hirschmuller (2008). The "classical" SGM algorithm has undergone two important changes in ASP® in order to include unrectified, larger images (NASA 2019): i) two-dimensional (2D) disparity search is performed, similarly to what is done in the Neighbor-Guided Semi-Global Matching algorithm (Xiang et al. 2016) and ii) ASP® uses a multi-resolution hierarchical search combined with a compressed memory scheme similar to what is used in the SGM algorithm (Rothermel et al. 2012). This SGM algorithm is based on multi-directional dynamic approaches. Even if it can be time-consuming because of significant memory requirements, SGM algorithm appears to be more effective in images with less texture and can discern finer resolution features than LSW since it tends to use much smaller matching kernels. However, SGM is prone to generate artefacts at tile boundaries and to produce inaccurate results in textureless regions. The ASP developers recommend using it cautiously in order to minimize these drawbacks (NASA 2019).
- More Global Matching/Smooth Semi-Global Matching (MGM/SSGM): introduced in Facciolo, Franchis, and Meinhardt (2015), the MGM algorithm

(also called SSGM algorithm) reduces the amount of high-frequency artefacts in textureless regions in the output image but at the expense of a longer computing time. A hybrid SGM/MGM mode is also proposed in ASP® where MGM only is used for the final resolution level which obtains results somewhere between the pure SGM and MGM options (NASA 2019).

In ASP®, the cost-mode variable (Figure 5) allows the user to choose the cost function used during the correlation step:

- Normalized Correlation Coefficient (NCC) (cost mode 2): the traditional area-based matching cost is the square difference of the pixel intensities. NCC often accomplishes the matching cost aggregation. This is a window-based matching technique that accounts for compensating gain changes. The disparity is then determined by a local winner-take-all operation in a small search window and checking with a simple threshold. The last step is characterized by sub-pixel interpolation and other post processing (Hu et al. 2016).
- Census Transform (cost mode 3): it associates a binary string to each pixel that encodes whether or not the pixel has a smaller intensity than each of its neighbours. Not only does it store the intensity ordering but also the spatial structure of the local neighbourhood (Hirschmuller and Scharstein 2008). It performs well for outdoor environments with uncontrolled lighting. ASP® allows the application of census transform only with the SGM correlator (NASA, 2019).
- Ternary Census Transform (cost mode 4): A modification of the census transform, which is more stable on low contrast terrain. The difference of the two census transform matching costs lies in the encoding of the results. For any given

rectangular window, a pixel will be encoded into a bit string in the Census Transform and into two bits in the Ternary Census Transform (Hu et al. 2016).

In MicMac®, the Malt tool proposes two semi-global matching algorithms, where the choice of the cost function is included in the step performed to choose a matching algorithm (Rupnik et al. 2020) (Figures 4 and 5):

- UrbanMNE is for a matching adapted to the urban digital elevation model. It handles matching in ground geometry, adapted to a scene that can be described by a single function $Z = f(X,Y)$ (where $X$, $Y$, $Z$ are Euclidean coordinates). Having the output geometry equal to the input geometry, UrbanMNE is perfectly adequate for modelling quasi-planar objects.

- GeomImage is for matching in ground image geometry (Rupnik, Pierrot-Deseilligny, and Delorme 2018). In this case, matching is performed by using the 'ground image geometry', which is more flexible and better suited for the modelling of fully 3D objects. With this mode, the geometry of the modelling is adapted to a selected point of view, consistent with the acquisition. In addition, Malt GeomImage handles a 'One-Two-Pixel multi-view image matching' (1-2 pixel matching) method, which is a new matching cost function that produces surfaces with enhanced resolution compared to the window-based semi-global matching technique, where the data term is replaced by a multi-view single pixel similarity measure, and a two-pixel window (Rupnik and Deseilligny 2019; Rupnik et al. 2020).

Because of different processing workflows, it could be difficult to standardize the processing parameters within the software itself and between software packages. We

tried to optimize the consistency of the comparison (Figure 5). As the area of interest corresponds to steep slopes, we used small correlation windows (5 × 5 pixels, 7 × 7 pixels, 9 × 9 pixels), but the small size of the windows may introduce more false matches or noise (NASA 2019). For LSW, a larger correlation kernel is used (15 × 15) due to its difficulty to find tie points on the cliff face. The regularization factor adds a constraint on the a priori position of the reconstructed points. The higher the factor, the more regular the result.

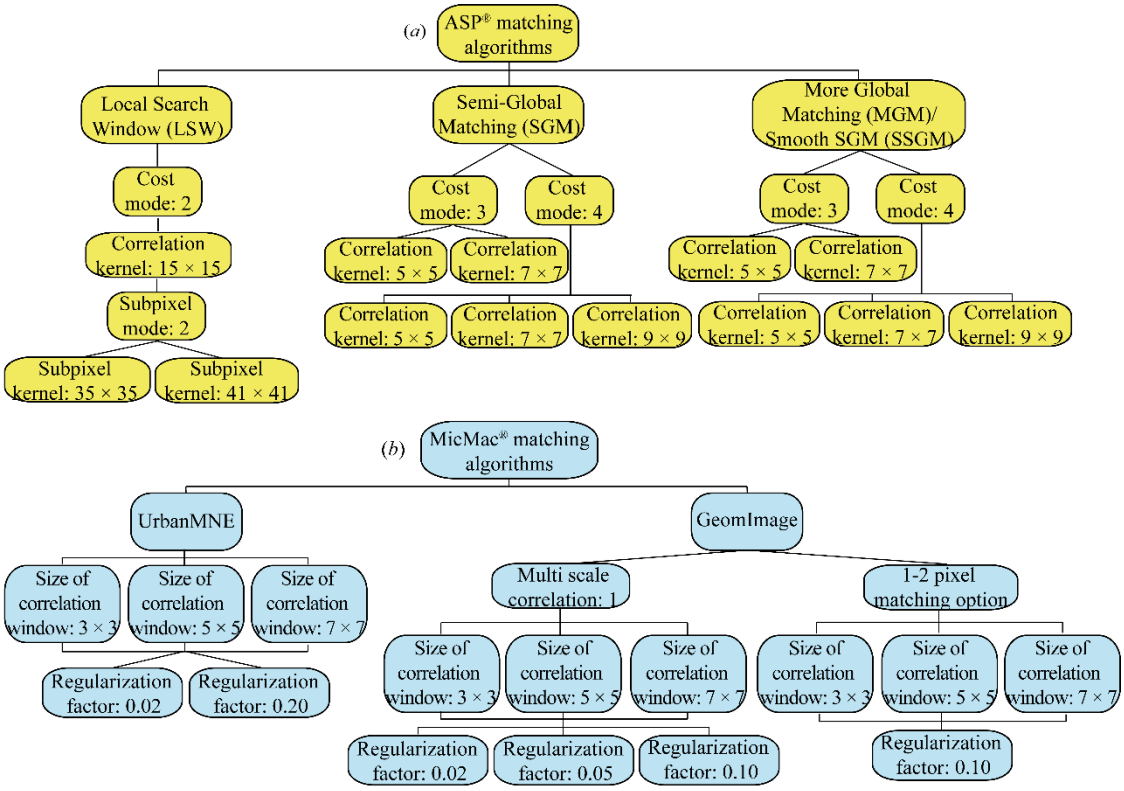


Figure 5. Parameters for the matching algorithms tested in (*a*) ASP® and (*b*) MicMac®.

While running MicMac® as ASP®, no Ground Control Points (GCPs) were provided. The Rational Polynomial Coefficients (RPCs) provide an approximate localization model used for geometric processing and orthorectification (ASTRIUM 2012). Bundle adjustment without GCPs ensure good results and do not introduce

undesirable deformations (Rupnik et al. 2016). Because of frequent georeferenced point clouds (coming from UAV or TLS) as ground truth data, the roughly georeferenced satellite point clouds are then realigned by Iterative Closest Point (ICP) co-registration algorithm (CloudCompare®).

*Quality Assessment*

A relative precision criterion is compulsory in order be able to assess the 3D reconstruction quality and therefore the relevance of our data to make single-source or multi-source comparisons (TLS data or UAV data). Thus, 3D reconstructions from the Pléiades images were filtered (artefact removal), georeferenced and compared to ground truth data at Varengeville-sur-Mer, acquired on 26 June 2017 using UAV. These synchronous surveys (UAV and satellites) allow to limit errors due to erosion events. The UAV and Pléiades point clouds were cut in order to have the same spatial extent (53700 m²) and the UAV point cloud was subsampled at 5 cm. A semi-automatic co-registration (ICP in CloudCompare®) using a rigid-body transform was performed to georeference the Pléiades point clouds by fitting on the UAV mesh (considered as the reference). This co-registration is efficiently constrained vertically (shore platform, plateau) and alongshore. Thus, the precision error of the Pléiades 3D reconstructions is assessed in comparison with Root Mean Square Error (RMSE in m) of the co-registration. Precision error is assessed in the cross-shore direction (which is the direction of erosion on the cliff face), based on the relative distance (normal of the cliff face) after fitting.

The georeferencing error (absolute error) is of lesser importance because we have frequent perfectly georeferenced and very high resolution surveys (TLS or UAV) that allow to align the point clouds coming from the Pléiades images.

## Results

### *Criteria for 3D reconstruction ranking*

Based on 146 tests performed with ASP® and MicMac® on different pairs of images, we sorted our results based on the:

- Relative precision in comparison with UAV data (mean distance which allows to calculate the distance relative to the mesh of the UAV data, and standard deviation to assess point dispersion);
- Point density of the clouds;
- Quality assessment of the reconstructions (not satisfactory, few satisfactory, satisfactory) taking into account the homogeneity of the reconstructed point distribution over the cliff face, artefacts and noise (Figure 6). Satisfactory reconstructions provide visibility of structural discontinuities from the cliff foot to the cliff top in order to observe rockfalls irrespective of their locations over the cliff face.

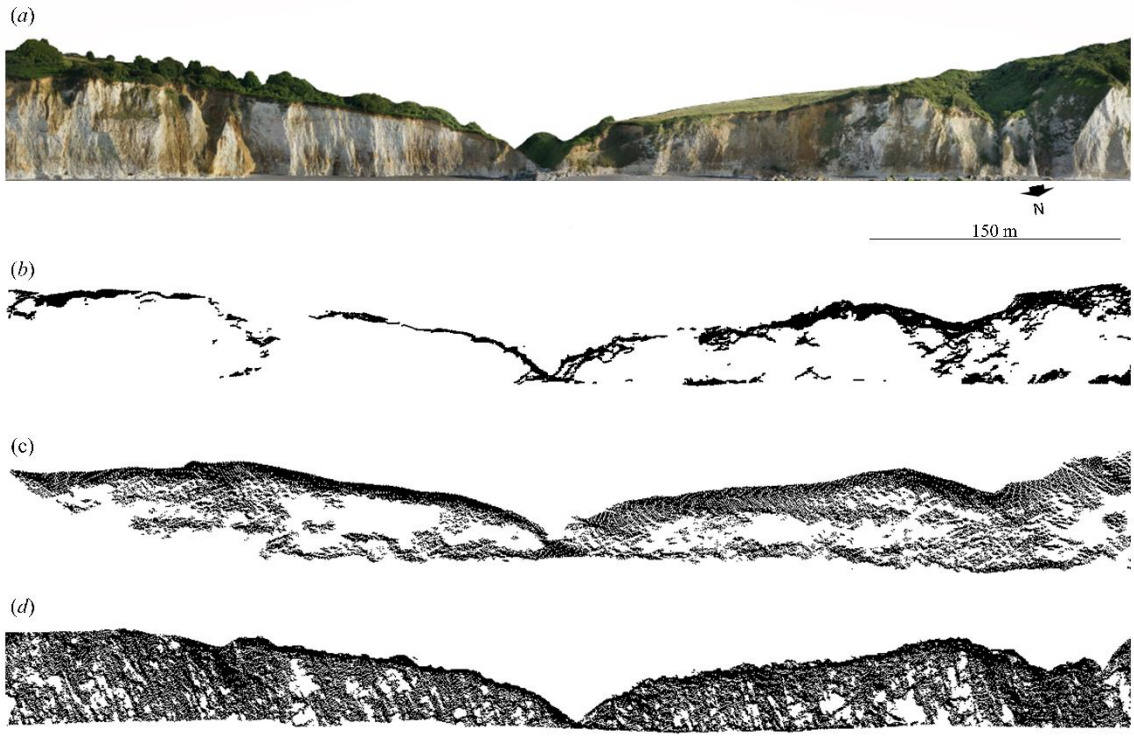


Figure 6. Cliff face reconstructed from UAV data (RICOCHET project, 26 June 2017) (*a*) and quality ranking of the 3D reconstructions from Pléiades images at Varengeville-sur-Mer: (*b*) not satisfactory result (10 June 2017 and 15 June 2017 at 40°, MicMac®, UrbanMNE, size of correlation window: 5 × 5, regularization factor: 0.20), (*c*) few satisfactory result (10 June 2017 and 15 June 2017 at 40°, ASP®, Local Search Window, cost mode: 2, correlation kernel: 15 × 15, subpixel kernel: 41 × 41), (*d*) satisfactory result (10 June 2017 and 15 June 2017 at 40°, MicMac®, GeomImage, multi scale correlation: 1, size of correlation window: 3 × 3, regularization factor: 0.05).

Unsurprisingly, and regardless of the software used, satisfactory reconstructions (48/146) have a minimum of one image with an incidence angle of 40°. When the 3D reconstruction uses two images with angles of 0° to 10°, the cliff face reconstruction is, at best, assessed as 'few satisfactory', i.e. with noise, artefacts or holes (Table 1) due to the acquisition geometry which is not adapted to the sub-vertical cliff face (Jaud et al. 2019; Letortu et al. 2020). There are more satisfactory reconstructions of the cliff face when the stereo restitution uses two images with an angle of 40°.

Among the 146 tests, the best 3D reconstruction per image pair was selected based on the three parameters described below. The objective was to select a satisfactory 3D reconstruction, with the best compromise between low mean distance and standard deviation values, and a high point density value (Table 1). The best reconstructions were selected and there are ten (Table 2). Taking only the mean error and standard deviation values into account, the reconstructions from the 0° to 10° datasets may seem more precise than the 40° stereo pairs, but in reality, this is weighted by the fact that most of the points reconstructed at 0° to 10° are located on the top of the cliff and less on the cliff face.

Table 1. Extract of the original table of the 146 tests with the selection of the best 3D reconstruction per pair (e.g. 10 June 2017 and 15 June 2017 at 40° using MicMac®).

Letortu P., Jaud M., Taouki M, Costa S., Maquaire O., Delacourt C., 2021. Three-dimensional (3D) reconstructions of the coastal cliff face in Normandy (France) based on oblique Pléiades imagery: assessment of Ames Stereo Pipeline® (ASP®) and MicMac® processing chains. *International Journal of Remote Sensing*. https://doi.org/10.1080/01431161.2021.1892857

| Software | Date of image pair | Angle of Incidence (°) | Matching algorithm | Specifications of each sofware ASP®: cost mode / correlation kernel (subpixel kernel) MicMac®: size of correlation window / regularization parameter | Point density (number of points m$^{-2}$) | Mean distance (m) | Standard deviation (m) | Quality assessment of 3D reconstruction (**the best one per pair in bold**) |
|---|---|---|---|---|---|---|---|---|
| MicMac® | 10 June 2017 and 15 June 2017 | 40 | UrbanMNE | 3 × 3 / 0.02 | 0.44 | -0.17 | 4.54 | not satisfactory |
| | | 40 | UrbanMNE | 3 × 3 / 0.20 | 0.44 | 0.22 | 2.92 | not satisfactory |
| | | 40 | UrbanMNE | 5 × 5 / 0.02 | 0.53 | 0.07 | 2.99 | not satisfactory |
| | | 40 | UrbanMNE | 5 × 5 / 0.20 | 0.47 | 0.29 | 3.74 | not satisfactory |
| | | 40 | UrbanMNE | 7 × 7 / 0.02 | 0.52 | 0.08 | 3.17 | not satisfactory |
| | | 40 | UrbanMNE | 7 × 7 / 0.20 | 0.47 | 0.20 | 3.13 | not satisfactory |
| | | 40 | GeomImage (CorsMS: 1) | 3 × 3 / 0.02 | 1.64 | -0.07 | 2.60 | satisfactory |
| | | 40 | GeomImage (CorsMS:1) | 3 × 3 / 0.05 | 1.71 | 0.00 | 2.37 | satisfactory |
| | | 40 | GeomImage (CorsMS: 1) | 3 × 3 / 0.10 | 1.72 | 0.15 | 2.12 | satisfactory |
| | | 40 | GeomImage (CorsMS: 1) | 5 × 5 / 0.02 | 1.83 | 0.13 | 2.20 | satisfactory |
| | | 40 | GeomImage (CorsMS: 1) | 5 × 5 / 0.05 | 1.84 | 0.16 | 2.30 | satisfactory |
| | | 40 | GeomImage (CorsMS: 1) | 5 × 5 / 0.10 | 1.82 | 0.19 | 2.28 | satisfactory |
| | | 40 | GeomImage (CorsMS: 1) | 7 × 7 / 0.02 | 1.76 | 0.08 | 2.12 | satisfactory |
| | | 40 | GeomImage (CorsMS: 1) | 7 × 7 / 0.05 | 1.81 | -0.09 | 2.06 | satisfactory |
| | | 40 | GeomImage (CorsMS: 1) | 7 × 7 / 0.10 | 1.79 | -0.09 | 2.03 | satisfactory |
| | | 40 | GeomImage (one-two pixel matching) | 3 × 3 / 0.10 | 1.70 | -0.05 | 1.83 | **satisfactory** |
| | | 40 | GeomImage (one-two pixel matching) | 5 × 5 / 0.10 | 1.75 | -0.08 | 1.92 | satisfactory |
| | | 40 | GeomImage (one-two pixel matching) | 7 × 7 / 0.10 | 1.67 | 0.14 | 2.46 | satisfactory |

399

Table 2. The best cliff face 3D reconstructions per image pair based on 146 tests

| Software | Date of image pair | Angle of Incidence (°) | Matching algorithm | Specifications of each sofware<br>ASP®: cost mode / correlation kernel<br>MicMac®: size of correlation window / regularization parameter | Point density (number of points $m^{-2}$) | Mean distance (m) | Standard deviation (m) | Quality assessment of 3D reconstruction |
|---|---|---|---|---|---|---|---|---|
| ASP® | 10 June 2017 and 15 June 2017 | 40 | MGM/SSGM | 3 / 7 × 7 | 0.93 | 0.01 | 2.97 | satisfactory |
| | 10 June 2017 and 15 June 2017 | 0 to 10 | MGM/SSGM | 4 / 7 × 7 | 0.89 | 0.06 | 2.94 | few satisfactory |
| | 10 June 2017 | 0 to 10 / 40 | MGM/SSGM | 4 / 7 × 7 | 0.49 | -0.30 | 2.50 | satisfactory |
| | 15 June 2017 and 06 July 2017 | 40 | MGM/SSGM | 3 / 7 × 7 | 0.95 | 0.13 | 1.91 | satisfactory |
| | 15 June 2017 and 06 July 2017 | 0 to 10 | MGM/SSGM | 3 / 5 × 5 | 0.50 | 0.07 | 1.68 | few satisfactory |
| MicMac® | 10 June 2017 and 15 June 2017 | 40 | GeomImage (1-2 pixel matching) | 3 × 3 / 0.1 | 1.70 | -0.05 | 1.83 | satisfactory |
| | 10 June 2017 and 15 June 2017 | 0 to10 | GeomImage (1-2 pixel matching) | 3 × 3 / 0.1 | 1.46 | 0.06 | 1.21 | few satisfactory |
| | 10 June 2017 | 0 to 10 / 40 | GeomImage (1-2 pixel matching) | 7 × 7 / 0.1 | 1.61 | 0.07 | 1.96 | satisfactory |
| | 15 June 2017 and 06 July 2017 | 40 | GeomImage (1-2 pixel matching) | 3 × 3 / 0.1 | 1.79 | 0.11 | 1.38 | satisfactory |
| | 15 June 2017 and 06 July 2017 | 0 to10 | GeomImage (CorsMS: 1) | 3 × 3 / 0.2 | 1.28 | -0.06 | 1.72 | few satisfactory |

### *Identification of the best image processing chain for the 3D cliff face reconstruction*

The comparison is made on the satisfactory results obtained with ASP® and with MicMac® (Table 2). The precision of the cliff face reconstruction is slightly better with MicMac® than with ASP® (average relative distance of 0.04 m and -0.05 m, respectively) along with the standard deviation, which is lower with MicMac® than with ASP® (average standard deviation of 1.72 m and 2.46 m, respectively). Furthermore, point clouds with MicMac® present a higher density (1.57 point $m^{-2}$ on average) than with ASP® (0.75 point $m^{-2}$ on average). With a better average precision associated with a lower error dispersion on the cliff face and a higher point density, the 3D reconstruction with MicMac® provides the most reliable dataset.

The relative differences in the 3D restitution from the image sets at 40° are distributed randomly over the entire cliff face (Figure 7). These are mainly artefacts or noise that

have not been removed during manual filtering.

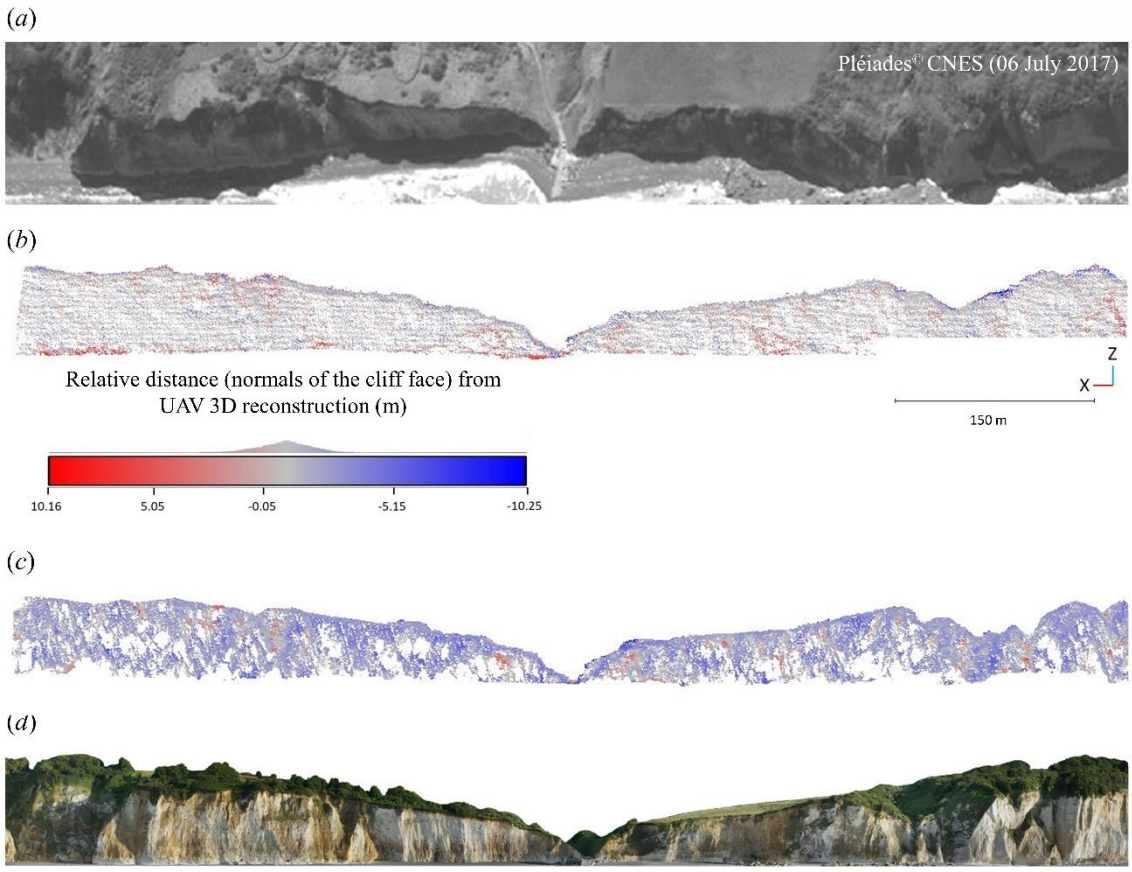


Figure 7. Relative distance of the cliff face normals (in m) at Varengeville-sur-Mer between the 3D reconstructions (stereoscopic pair on 15 June 2017 and (*a*) 06 July 2017 at 40°) with (*b*) ASP® (More Global Matching, cost mode: 3, correlation kernel: 7 × 7) and (*c*) MicMac® (GeomImage, size of correlation window: 3 × 3, regularization parameter: 0.10) compared with (*d*) UAV 3D reconstruction (26 June 2017).

Per software programme, the best processing chain is (Table 2, Figure 8):

- In ASP®: MGM/SSGM matching algorithm, with a cost mode 3 or 4 and a correlation kernel of 7 × 7.
- In MicMac®: GeomImage (1-2 pixel matching) matching algorithm with a correlation window size of 3 × 3 or 7 × 7, associated with a regularization parameter of 0.10.

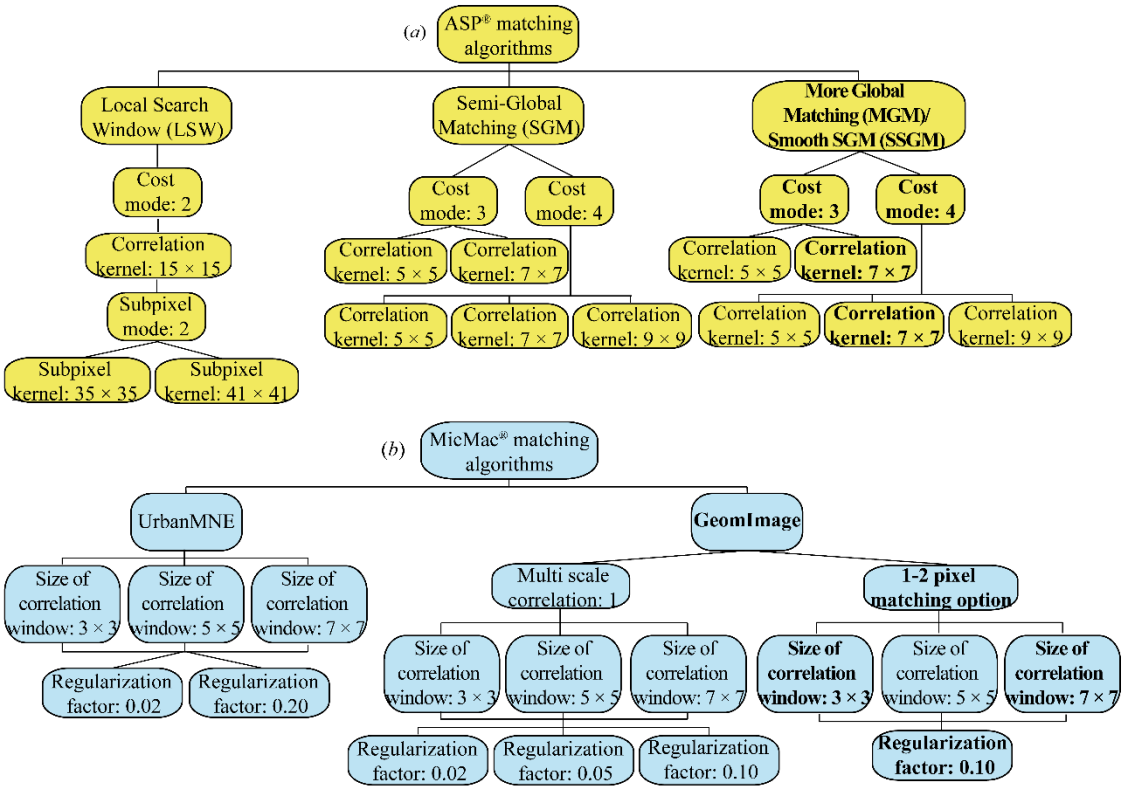


Figure 8. Best parameters (in bold) for satisfactory 3D reconstructions of the cliff face at Varengeville-sur-Mer with (*a*) ASP® and (*b*) MicMac®.

In MicMac®, GeomImage matching algorithm has better results than UrbanMNE one due to the topography of the cliff face and the acquisition geometry. As illustrated in Figure 8, the SGM methods provide better results as they are solved with multi-directional dynamic programming techniques, and thereby do not impose any constraints on the regularity term. The optimization is thus resolved along independent lines of pixels. These approaches provide robust reconstructions within a reasonable processing time (around 30 min for images of 1 million pixels). The reconstructed surfaces are morphologically preserved because the template windows chosen are small (3 × 3, 7 × 7) in the optimization process. In the SGM approach, occlusions are typically predicted by performing a symmetric consistency check in a stereo pair.

## Discussion

### *Potential of this approach for diachronic monitoring*

The presented dataset is rather original and challenging given its unusual configuration (high imaging angle, multiple dates) and the fact that the images present shadows over the area of interest. Thus, this study highlights the flexibility of the tested processing chains.

At this stage, a first quantification of the eroded volume can be estimated by using a 'satisfactory' cliff face reconstruction and an older dataset collected in 2015 using TLS. A difference was calculated between the point cloud of the stereoscopic pair on 10 June 2017 and 15 June 2017 at 40° and the TLS mesh collected on 25 September 2015. On the eastern part of the cliff face, where there is an erosion area, the Pléiades-TLS comparison calculates an eroded volume of 796.5 $m^3$ for a surface area spanning 4752.5 $m^2$. This calculation is then compared with the result of the differences between the TLS mesh (25 September 2015) and the UAV point cloud (26 June 2017) which leads to an eroded volume of 1134.4 $m^3$ (over the same surface, knowing that the surface affected by the rockfall is of 543 $m^2$) (Figure 9). The difference in the two volumetric estimations demonstrates that it is possible to quantify erosion by using Pléiades satellite photogrammetry within a margin of error of approximately 0.071 $m^3$ $m^{-2}$.

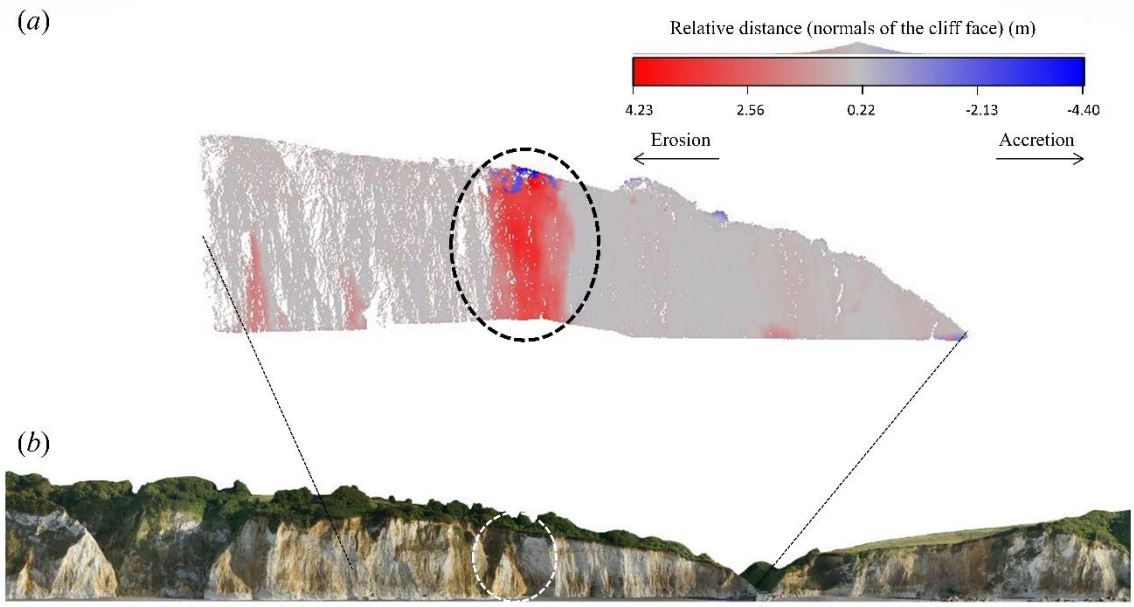


Figure 9. (*a*) Relative distance (m) of the cliff face between the TLS mesh (25 September 2015) and (*b*) the UAV data (26 June 2017) with detected erosion at Varengeville-sur-Mer.

For highly erosive areas, high angle of incidence images from the Pléiades satellites provide a new approach for a first order quantification of erosion on large portions of cliff lines (in line with the hydro-sedimentary cell), with high repeatability, satisfactory resolution and precision, and at low cost. This method therefore provides major opportunities for improving the knowledge about coastal cliff dynamics thanks to the rockfall detection threshold assessed at 100 $m^3$, which corresponds to 69% of rockfalls censed around the study area (Letortu et al. 2015). The creation of a considerable rockfall database on large stretches of coasts is thus possible, which could help to better understand rockfall triggers and, ultimately, to protect people (Naylor, Stephenson, and Trenhaile 2010).

### *Contribution of tri-stereo reconstruction*

MicMac® gives the best results in stereoscopic reconstruction and, unlike ASP®, it can also be used to perform tri-stereoscopic reconstructions. Eighteen tri-stereo tests were carried out with MicMac® from images with an incidence angle of 40° (10 June 2017, 15 June 2017 and 18 June 2017, Table 3), they are mostly satisfactory (11/18). Compared with stereoscopic pairs, the point density is slightly higher with a stereoscopic triplet (1.82 point $m^{-2}$ versus 1.70 point $m^{-2}$), the mean distance is lower (0.01 m versus 0.04 m) but has a higher data dispersion (standard deviation of 2.14 m versus 1.72 m) due to the presence of a higher number of artefacts.

Table 3. 3D reconstruction tests based on tri-stereo matching in MicMac® (triplet images: 10 June 2017-15 June 2017-18 June 2017).

| Date of image triplet at 40° | Tri-stereo matching algorithm | Size of correlation window / regularization parameter | Point density (number of points $m^{-2}$) | Mean distance (m) | Standard deviation (m) | Quality assessment of 3D reconstruction (**the best one in bold**) |
|---|---|---|---|---|---|---|
| 10 June 2017, 15 June 2017 and 18 June 2017 | UrbanMNE | 3 × 3 / 0.02 | 0.48 | 0.38 | 4.18 | not satisfactory |
| | UrbanMNE | 3 × 3 / 0.20 | 0.38 | 0.15 | 2.82 | not satisfactory |
| | UrbanMNE | 5 × 5 / 0.02 | 0.45 | 0.42 | 3.11 | not satisfactory |
| | UrbanMNE | 5 × 5 / 0.20 | 0.35 | 0.78 | 3.99 | not satisfactory |
| | UrbanMNE | 7 × 7 / 0.02 | 0.47 | 0.20 | 2.71 | not satisfactory |
| | UrbanMNE | 7 × 7 / 0.20 | 0.39 | 0.25 | 2.94 | not satisfactory |
| | GeomImage (CorsMS: 1) | 3 × 3 / 0.02 | 2.31 | 0.31 | 3.21 | satisfactory |
| | GeomImage (CorsMS: 1) | 3 × 3 / 0.05 | 1.98 | -0.05 | 2.45 | satisfactory |
| | GeomImage (CorsMS: 1) | 3 × 3 / 0.10 | 1.72 | 0.06 | 1.54 | **satisfactory** |
| | GeomImage (CorsMS: 1) | 5 × 5 / 0.02 | 1.71 | 0.08 | 1.51 | satisfactory |
| | GeomImage (CorsMS: 1) | 5 × 5 / 0.05 | 1.70 | 0.07 | 1.50 | satisfactory |
| | GeomImage (CorsMS: 1) | 5 × 5 / 0.10 | 1.98 | -0.06 | 2.75 | satisfactory |
| | GeomImage (CorsMS: 1) | 7 × 7 / 0.02 | 1.66 | 0.09 | 1.54 | satisfactory |
| | GeomImage (CorsMS: 1) | 7 × 7 / 0.05 | 1.63 | 0.10 | 1.52 | satisfactory |
| | GeomImage (CorsMS: 1) | 7 × 7 / 0.10 | 1.58 | 0.13 | 1.57 | satisfactory |
| | GeomImage (1-2 pixel matching) | 3 × 3 / 0.10 | 1.97 | -0.35 | 3.31 | satisfactory |
| | GeomImage (1-2 pixel matching) | 5 × 5 / 0.10 | 1.72 | 0.05 | 1.74 | satisfactory |
| | GeomImage (1-2 pixel matching) | 7 × 7 / 0.10 | 1.89 | -0.33 | 3.06 | few satisfactory |

## Conclusions

As previously mentioned (Jaud et al. 2019; Letortu et al. 2020), a stereo restitution of the cliff face based on images with an angle of incidence of 0° to 10° appears not adapted to the sub-vertical slope (70° to 90°) whereas images with an angle of incidence

493 of 40° allow satisfactory results to be achieved. Between ASP® and MicMac®, the best
494 open-source stereo restitution software to use high angle incidence and multi-date
495 images is MicMac® and the best performance is obtained using GeomImage (1-2 pixel
496 matching) with a size of correlation window of 3 × 3 or 7 × 7 associated with a
497 regularization parameter of 0.10. With these parameters, 3D cliff face reconstructions
498 have an average point density of 1.70 point $m^{-2}$, a mean distance from UAV ground
499 truth data of 0.04 m and a standard deviation of 1.72 m. The ASP® software with the
500 MGM/SSGM stereo matching algorithm is the second-best option, with cost mode 3 or
501 4 and a correlation kernel of 7 × 7. These parameters provide point clouds with an
502 average point density of 0.79 point $m^{-2}$, a mean distance of -0.06 m and a standard
503 deviation of 2.46 m. These point cloud characteristics used in a diachronic approach can
504 detect rockfalls above 100 $m^3$, which includes the large majority of rockfalls (69%)
505 around the study area (Letortu et al. 2015). Pléiades oblique images appear to be a great
506 opportunity for monitoring cliff faces, for quantifying erosion over large spans of
507 coastline and for creating a rockfall database which could help to better understand
508 rockfall triggers (in order to people prevention/protection).

509 Future projects aim at developing new approaches to optimize the detection and
510 quantification of cliff face erosion using Pléiades images (including the Pléiades Neo
511 constellation that will be launched in 2021 and 2022, with a spatial resolution of
512 panchromatic images of 0.30 m at the nadir). To achieve this goal, images should have
513 an angle of incidence from 20° to 30° (the best imaging angles for cliff face survey
514 (Jaud et al. 2019) when cliffs have a sub-vertical slope (70° to 90°) as in Varengeville-
515 sur-Mer) and should be acquired in a favourable environment (few cloud cover and cliff
516 face orientation parallel to the Pléiades orbit). About the method, instead of relying on a
517 3D reconstruction of the entire cliff face by stereo- and tri-stereo restitution, new

518 methods will be based on a prior change detection on the cliff face in order to identify
519 erosion areas. A diachronic 3D reconstruction of these areas should improve the
520 quantification of the cliff erosion.

521 **Author Contributions**

522 Pauline Letortu and Marion Jaud conceived and designed the data acquisition and data
523 analysis methods. Roza Taouki processed the images. Roza Taouki, Marion Jaud and
524 Pauline Letortu contributed to the data analysis. Pauline Letortu, Roza Taouki and
525 Marion Jaud wrote and illustrated the paper. Stéphane Costa and Olivier Maquaire
526 organized the UAV survey, used as ground truth data. Pauline Letortu, Marion Jaud and
527 Christophe Delacourt are responsible for the project administration.

528 **Funding**

529 This research was supported by the CNES (EROFALITT project). It is based on
530 observations with the Pléiades satellites. This work was also funded by the ISblue
531 project, the Interdisciplinary graduate school for the blue planet (ANR-17-EURE-0015),
532 and was co-funded via a grant from the French government under the 'Investissements
533 d'Avenir' programme. This work was also supported by the ANR project 'RICOCHET:
534 multi-risk assessment on coastal territory in a global change context' funded by the
535 French Research National Agency [ANR-16-CE03-0008].

536 **Acknowledgments**

537 This work is also part of the Service National d'Observation DYNALIT, via the
538 research infrastructure ILICO. The Pléiades images are subject to copyright: Pléiades©
539 CNES, Distribution Astrium Services.

## References

ASTRIUM. 2012. *Pléiades Imagery - User Guide*. Technical report USRPHR-DT-125-SPOT-2.0.

Bagnardi, Marco, Pablo J. González, and Andrew Hooper. 2016. "High-Resolution Digital Elevation Model from Tri-Stereo Pleiades-1 Satellite Imagery for Lava Flow Volume Estimates at Fogo Volcano." *Geophysical Research Letters* 43 (12). Wiley Online Library: 6267–6275.

Berthier, E., C. Vincent, E. Magnússon, á. þ. Gunnlaugsson, P. Pitte, E. Le Meur, M. Masiokas, et al. 2014. "Glacier Topography and Elevation Changes Derived from Pléiades Sub-Meter Stereo Images." *The Cryosphere* 8 (6): 2275–2291. doi:10.5194/tc-8-2275-2014.

Collin, Antoine, James L. Hench, Yves Pastol, Serge Planes, Lauric Thiault, Russell J. Schmitt, Sally J. Holbrook, Neil Davies, and Matthias Troyer. 2018. "High Resolution Topobathymetry Using a Pleiades-1 Triplet: Moorea Island in 3D." *Remote Sensing of Environment* 208 (April): 109–119. doi:10.1016/j.rse.2018.02.015.

Costa, Stéphane. 1997. "Dynamique Littorale et Risques Naturels : L'impact Des Aménagements, Des Variations Du Niveau Marin et Des Modifications Climatiques Entre La Baie de Seine et La Baie de Somme (Haute-Normandie, Picardie; France)." Paris 1. http://www.theses.fr/1997PA010522.

Costa, Stéphane, Olivier Maquaire, Pauline Letortu, Guillaume Thirard, Vincent Compain, Thomas Roulland, Mohand Medjkane, et al. 2019. "Sedimentary Coastal Cliffs of Normandy: Modalities and Quantification of Retreat." *Journal of Coastal Research* 88 (SI): 46–60. doi:10.2112/SI88-005.1.

Facciolo, Gabriele, Carlo De Franchis, and Enric Meinhardt. 2015. "MGM: A Significantly More Global Matching for Stereovision." In . doi:10.5244/C.29.90.

Foyle, A.M., and M.D. Naber. 2012. "Decade-Scale Coastal Bluff Retreat from LiDAR Data: Lake Erie Coast of NW Pennsylvania, USA." *Environmental Earth Sciences* 66 (7): 1999–2012. doi:10.1007/s12665-011-1425-x.

Gulyaev, S.A., and J.S. Buckeridge. 2004. "Terrestrial Methods for Monitoring Cliff Erosion in an Urban Environment." *Journal of Coastal Research* 20 (3): 871–878.

Hartley, Richard, and Andrew Zisserman. 2003. *Multiple View Geometry in Computer Vision*. Cambridge University Press.

Hirschmuller, Heiko. 2008. "Stereo Processing by Semiglobal Matching and Mutual Information." *IEEE Transactions on Pattern Analysis and Machine Intelligence* 30 (2): 328–341. doi:10.1109/TPAMI.2007.1166.

Hirschmuller, Heiko, and Daniel Scharstein. 2008. "Evaluation of Stereo Matching Costs on Images with Radiometric Differences." *IEEE Transactions on Pattern Analysis and Machine Intelligence* 31 (9). IEEE: 1582–1599.

Hu, Han, Chongtai Chen, Bo Wu, Xiaoxia Yang, Qing Zhu, and Yulin Ding. 2016. "Texture-Aware Dense Image Matching Using Ternary Census Transform." *ISPRS Annals of the Photogrammetry, Remote Sensing and Spatial Information Sciences*. Copernicus Publications.

Jaud, Marion, Pauline Letortu, Claire Théry, Philippe Grandjean, Stéphane Costa, Olivier Maquaire, Robert Davidson, and Nicolas Le Dantec. 2019. "UAV Survey of a Coastal Cliff Face - Selection of the Best Imaging Angle." *Measurement* 139: 10–20. doi:10.1016/j.measurement.2019.02.024.

588 Letortu, P., S. Costa, A. Bensaid, J.-M. Cador, and H. Quénol. 2014. "Vitesses et
589 Modalités de Recul Des Falaises Crayeuses de Haute-Normandie (France):
590 Méthodologie et Variabilité Du Recul." *Geomorphologie: Relief, Processus,*
591 *Environnement* 20 (2): 133–144. doi:10.4000/geomorphologie.10872.
592 Letortu, P., S. Costa, J.-M. Cador, C. Coinaud, and O. Cantat. 2015. "Statistical and
593 Empirical Analyses of the Triggers of Coastal Chalk Cliff Failure." *Earth*
594 *Surface Processes and Landforms* 40 (10): 1371–1386. doi:10.1002/esp.3741.
595 Letortu, Pauline, Stéphane Costa, Olivier Maquaire, and Robert Davidson. 2019.
596 "Marine and Subaerial Controls of Coastal Chalk Cliff Erosion in Normandy
597 (France) Based on a 7-Year Laser Scanner Monitoring." *Geomorphology* 335
598 (June): 76–91. doi:10.1016/j.geomorph.2019.03.005.
599 Letortu, Pauline, Marion Jaud, Philippe Grandjean, Jérôme Ammann, Stéphane Costa,
600 Olivier Maquaire, Robert Davidson, Nicolas Le Dantec, and Christophe
601 Delacourt. 2018. "Examining High-Resolution Survey Methods for Monitoring
602 Cliff Erosion at an Operational Scale." *GIScience & Remote Sensing* 55 (4):
603 457–476. doi:10.1080/15481603.2017.1408931.
604 Letortu, Pauline, Marion Jaud, Claire Théry, Jean Nabucet, Roza Taouki, Sophie Passot,
605 and Emmanuel Augereau. 2020. "The Potential of Pléiades Images with High
606 Angle of Incidence for Reconstructing the Coastal Cliff Face in Normandy
607 (France)." *International Journal of Applied Earth Observation and*
608 *Geoinformation* 84: 101976.
609 Michoud, C., D. Carrea, S. Costa, M.H. Derron, M. Jaboyedoff, C. Delacourt, O.
610 Maquaire, P. Letortu, and R. Davidson. 2014. "Landslide Detection and
611 Monitoring Capability of Boat-Based Mobile Laser Scanning along Dieppe
612 Coastal Cliffs, Normandy." *Landslides* 12 (2): 403–418. doi:10.1007/s10346-
613 014-0542-5.
614 Mortimore, R.N., K.J. Stone, J. Lawrence, and A. Duperret. 2004. "Chalk Physical
615 Properties and Cliff Instability." In *Coastal Chalk Cliff Instability*, 20:75–88.
616 Geological Society Engineering Geology Special Publication.
617 NASA. 2019. *The Ames Stereo Pipeline: NASA's Open Source Automated*
618 *Stereogrammetry Software*. Version 2.6.2. NASA.
619 Https://ti.arc.nasa.gov/tech/asr/groups/intelligent-
620 robotics/ngt/stereo/#Documentation.
621 Naylor, L.A., W.J. Stephenson, and A.S. Trenhaile. 2010. "Rock Coast
622 Geomorphology: Recent Advances and Future Research Directions."
623 *Geomorphology* 114 (1–2): 3–11. doi:10.1016/j.geomorph.2009.02.004.
624 Pédelaborde, Pierre. 1958. *Le Climat Du Bassin Parisien : Essai d'une Méthode*
625 *Rationnelle de Climatologie Physique*. Vol. 2.
626 Poli, D., F. Remondino, E. Angiuli, and G. Agugiaro. 2015. "Radiometric and
627 Geometric Evaluation of GeoEye-1, WorldView-2 and Pléiades-1A Stereo
628 Images for 3D Information Extraction." *ISPRS Journal of Photogrammetry and*
629 *Remote Sensing* 100 (February): 35–47. doi:10.1016/j.isprsjprs.2014.04.007.
630 Pomerol, B., H. W. Bailey, C. Monciardini, and R. N. Mortimore. 1987.
631 "Lithostratigraphy and Biostratigraphy of the Lewes and Seaford Chalks: A
632 Link across the Anglo-Paris Basin at the Turonian-Senonian Boundary."
633 *Cretaceous Research* 8 (4): 289–304.
634 RIEGL Laser Measurement Systems. 2014. *Datasheet VZ-400*. RIEGL Laser
635 Measurement Systems GmbH. Austria.

636 Rothermel, Mathias, Konrad Wenzel, Dieter Fritsch, and Norbert Haala. 2012. "SURE:
637 Photogrammetric Surface Reconstruction from Imagery." In *Proceedings LC3D*
638 *Workshop, Berlin*. Vol. 8.
639 Rupnik, Ewelina, Mehdi Daakir, and Marc Pierrot Deseilligny. 2017. "MicMac – a
640 Free, Open-Source Solution for Photogrammetry." *Open Geospatial Data,*
641 *Software and Standards* 2 (1): 14. doi:10.1186/s40965-017-0027-2.
642 Rupnik, Ewelina, M. Pierrot Deseilligny, Arthur Delorme, and Yann Klinger. 2016.
643 "Refined Satellite Image Orientation in the Free Open-Source Photogrammetric
644 Tools APERO/MICMAC." *ISPRS Annals of the Photogrammetry, Remote*
645 *Sensing and Spatial Information Sciences* 3: 83.
646 Rupnik, Ewelina, and Marc Pierrot Deseilligny. 2019. *More Surface Detail with One-*
647 *Two-Pixel Matching*. Research Report. IGN - Laboratoire MATIS.
648 https://hal.archives-ouvertes.fr/hal-02371337.
649 Rupnik, Ewelina, M. Pierrot-Deseilligny, J.M. Muller, Zilin Zhou, Mehdi Daakir, and
650 G. Maillet. 2020. *MicMac, Apero, Pastis and Other Beverages in a Nutshell!*
651 https://github.com/micmacIGN/Documentation.
652 Rupnik, Ewelina, Marc Pierrot-Deseilligny, and Arthur Delorme. 2018. "3D
653 Reconstruction from Multi-View VHR-Satellite Images in MicMac." *ISPRS*
654 *Journal of Photogrammetry and Remote Sensing* 139 (May): 201–211.
655 doi:10.1016/j.isprsjprs.2018.03.016.
656 Shean, David E., Oleg Alexandrov, Zachary M. Moratto, Benjamin E. Smith, Ian R.
657 Joughin, Claire Porter, and Paul Morin. 2016. "An Automated, Open-Source
658 Pipeline for Mass Production of Digital Elevation Models (DEMs) from Very-
659 High-Resolution Commercial Stereo Satellite Imagery." *ISPRS Journal of*
660 *Photogrammetry and Remote Sensing* 116: 101–117.
661 Trzpit, JP. 1970. "Climat." In *Atlas de Normandie*, 2.
662 Xiang, Jiang, Ziyun Li, David Blaauw, Hun Seok Kim, and Chaitali Chakrabarti. 2016.
663 "Low Complexity Optical Flow Using Neighbor-Guided Semi-Global
664 Matching." In *2016 IEEE International Conference on Image Processing*
665 *(ICIP)*, 4483–4487. doi:10.1109/ICIP.2016.7533208.
666 Young, Adam P., and Jessica E. Carilli. 2019. "Global Distribution of Coastal Cliffs."
667 *Earth Surface Processes and Landforms* 44: 1309–1316. doi:10.1002/esp.4574.
668 Zhou, Yu, Barry Parsons, John R. Elliott, Ivana Barisin, and Richard T. Walker. 2015.
669 "Assessing the Ability of Pleiades Stereo Imagery to Determine Height Changes
670 in Earthquakes: A Case Study for the El Mayor-Cucapah Epicentral Area."
671 *Journal of Geophysical Research: Solid Earth* 120 (12). Wiley Online Library:
672 8793–8808.
673 Zviely, D., and M. Klein. 2004. "Coastal Cliff Retreat Rates at Beit-Yannay, Israel, in
674 the 20th Century." *Earth Surface Processes and Landforms* 29 (2): 175–184.
675 doi:10.1002/esp.1019.
676